

Cytotoxic and Molecular Docking Studies of *Camellia sinensis* Twig Extracts Against Human Cancer Cell Lines

Nayakanti Bhasker Babu^{1,2*}, Donakonda Madhuri²

¹*Research Scholar, JNTUA, Ananthapur, Andhra Pradesh.

²Creative Educational Society's College of Pharmacy, JNTUA, Kurnool, Andhra Pradesh, 518218.

*Presenting Author : bhasker.nayakanti@gmail.com

Abstract:

Camellia sinensis (green tea) is a rich source of polyphenolic phytochemicals with reported antioxidant and anticancer properties. The present study investigated the cytotoxic potential of different solvent extracts of *Camellia sinensis* twigs and explored their molecular interactions using in vitro and in silico approaches. Sequential extraction was carried out using methanol, butanol, hexane, and ethyl acetate. Cytotoxic activity was evaluated using the MTT assay against human breast cancer cell lines (MCF-7). In parallel, molecular docking studies were performed using Glide (Schrödinger) to predict the binding affinity of major green tea phytoconstituents against selected target proteins (PDB IDs: 6MTU and 6YQ4).

The results demonstrated that the methanolic and butanolic twig extracts exhibited significant cytotoxic activity against MCF-7 cells, with IC₅₀ values of $42.45 \pm 0.754 \mu\text{g/mL}$ and $36.05 \pm 0.614 \mu\text{g/mL}$, respectively, while ethyl acetate and hexane extracts showed comparatively lower activity. Molecular docking studies revealed strong binding interactions of catechin gallate and theaflavin derivatives with the selected protein targets, exhibiting docking scores superior to some standard anticancer drugs. The combined in vitro and in silico findings suggest that *Camellia sinensis* twig extracts possess promising anticancer potential. Further studies involving bioactive compound isolation, mechanistic evaluation, and in vivo validation are recommended to confirm their therapeutic applicability.

Keywords: *Camellia sinensis*, twig extracts, cytotoxicity, molecular docking, cancer cell lines, anticancer activity, apoptosis, phytochemicals, computational analysis, drug discovery.

1.1. Introduction:

Green tea is a type of tea that is made from *Camellia sinensis* leaves and buds that have not undergone the same withering and oxidation process which is used to make oolong teas and black teas. Green tea originated in China, and since then its production and manufacture has spread to other countries in East Asia. Polyphenols found in green tea include epigallocatechin gallate (EGCG), epicatechin gallate, epicatechins and flavanols, which are under laboratory research for their potential effects in vivo. Other components include three kinds of flavonoids, known as kaempferol, quercetin, and myricetin. (1) Although the mean content of flavonoids and catechins in a cup of green tea is higher than that in the same volume of other food and drink items that are traditionally considered to promote health, flavonoids and catechins have no proven biological effect in humans.

Green tea twigs are initially processed by soaking in an alcohol solution, which may be further concentrated to various levels; byproducts of the process are also packaged and used. Extracts are sold over the counter in liquid, powder, capsule, and tablet forms, and may contain up to 17.4% of their total weight in caffeine, though decaffeinated versions are also available.

Green tea extract is usable as a clean label food preservative, protecting fats from rancidity. The oil-soluble form used is palmitoylated green tea catechins, ruled generally recognized as safe in 2020.

Catechins are natural polyphenolic phytochemicals that exist in food and medicinal plants, such as tea, legume and rubiaceae. An increasing number of studies have associated the intake of catechins-rich foods with the prevention and treatment of chronic diseases in humans, such as inflammatory bowel disease (IBD) (3). Catechin plays an important role in the prevention of atherosclerosis progression due to vascular anti-inflammatory action, and the inhibition of vascular cell growth factors involved in atherosclerosis. Inhibition of thrombo genesis by catechin is due to the suppression of platelet adhesion. Epigallocatechin gallate (EGCG), also known as epigallocatechin-3-gallate, is the ester of epigallocatechin and gallic acid, and is a type of catechin. (4,5) Theaflavin is a chemical in black tea(6) that is formed from fermentation of green tea. It is used as medicine. People take theaflavin for high levels of cholesterol or other fats (lipids) in the blood (hyperlipidemia), heart disease, obesity, and cancer, but there is no good scientific evidence to support these uses.

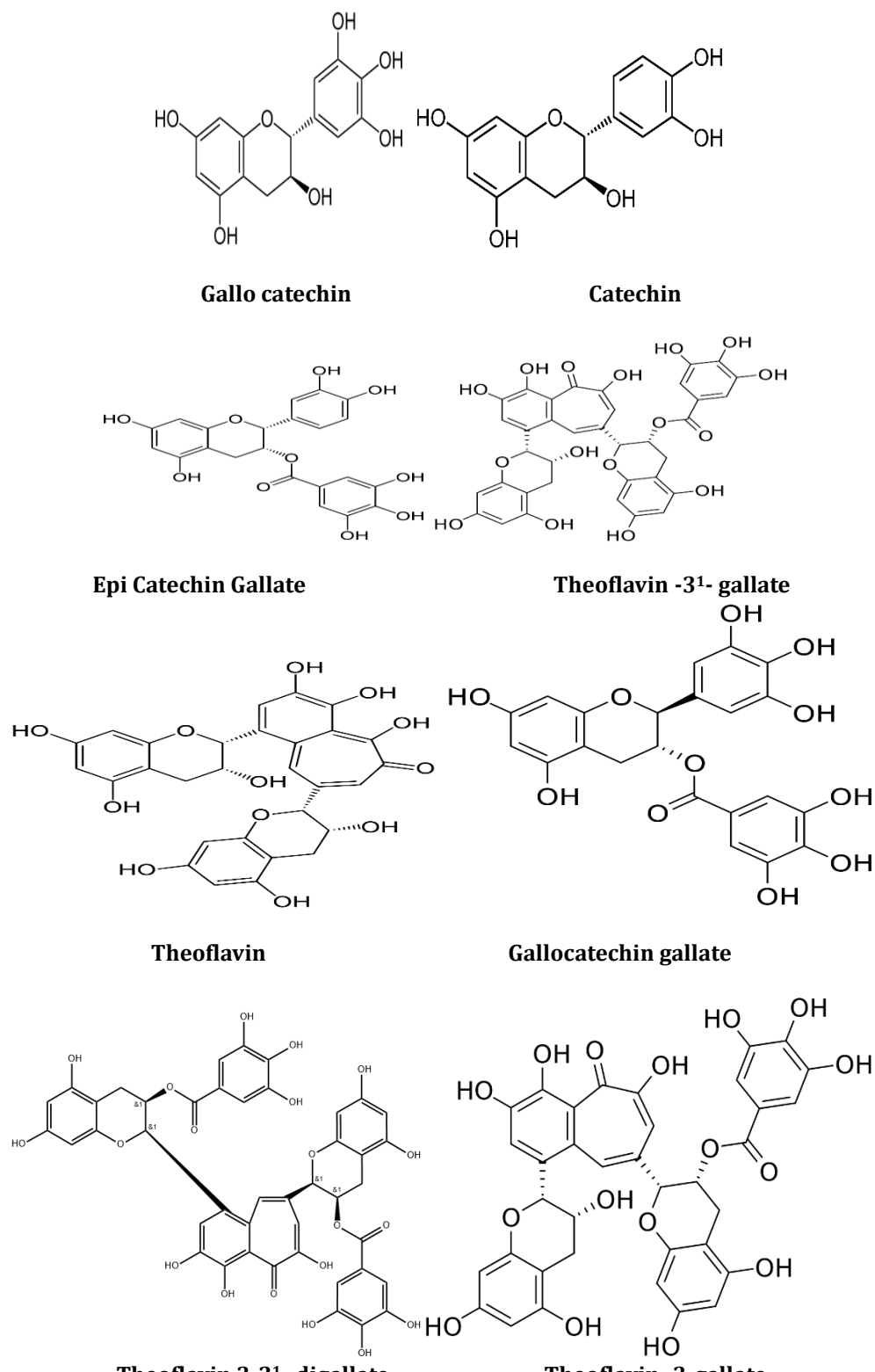


Figure No.1. Structures of components

1.2. Introduction to MTT Assay:

Measurement of cell viability and proliferation forms the basis for numerous in vitro assays of a cell population's response to external factors. The MTT Cell Proliferation Assay measures the cell

proliferation rate and conversely, when metabolic events lead to apoptosis or necrosis, the reduction in cell viability.

Molecular docking is a key tool in structural molecular biology and computer-assisted drug

design. The goal of ligand-protein docking is to predict the predominant binding mode(s) of a ligand with a protein of known three-dimensional structure. Successful docking methods search high-dimensional spaces effectively and use a scoring function that correctly ranks candidate dockings. Docking can be used to perform virtual screening on large libraries of compounds, rank the results, and propose structural hypotheses of how the ligands inhibit the target, which is invaluable in lead optimization. The setting up of the input structures for the docking is just as important as the docking itself, and analyzing the results of stochastic search methods can sometimes be unclear.

2 MATERIALS AND METHODS:

DMEM (Dulbecco's modified Eagles medium), MTT [3-(4,5-dimethylthiazol-2-yl)-2,5-diphenyl tetrazolium bromide], trypsin, EDTA Phosphate Buffered Saline (PBS) and were purchased from Sigma Chemicals Co. (St. Louis, MO) and Fetal Bovine Serum (FBS) were purchased from Gibco. 25 cm² and 75 cm² flask and 96 well plated purchased from Eppendorf India.

2.1 Maintenance of Cell Line:

The Cancer cell lines were purchased from NCCS, Pune and the cells were maintained in DMEM supplemented with 10 % FBS and the antibiotics penicillin/streptomycin (0.5 mL-1), in atmosphere of 5% CO₂ /95% air at 37 °C.

2.2. Molecular docking studies

- A molecular docking study was carried out to assess their interaction and binding modes with target receptors using Glide standard precision (SP) Maestro Schrodinger 2020_1.
- It is comprised of a series of steps which includes the selection of protein and its preparation, receptor grid generation, preparation of ligands, and its docking to the receptor.
- Protein with PDB ID 6MTU (Crystal structure of human Scribble PDZ1:pMCC complex), and 6YQ4 (Crystal structure of *Fusobacterium nucleatum* tannase) were downloaded from Protein Data Bank at a resolution of 2.14 Å, and 2.40 Å respectively.
- Both proteins were subjected to preprocessing, optimization, and minimization by the OPLS4 force

RESULTS AND DISCUSSION:

Table No.1.Docking Score and Interactions of Compounds against 6MTU Protein

S.No	Compound Name	Docking Score	Interactions
1	Catechin gallate	-7.15	THR749, PRO750, SEP828
2	Theoflavin-3-gallate	-6.91	THR749, SEP828
3	Theoflavin	-6.46	THR749, TYR751, GLU826, SEP828
4	Theoflavin3-3'-digallate	-6.42	SER761, GLU826, SEP828

field with the help of the protein preparation wizard.

- The binding pocket / active site was identified by site map analysis and chosen top site (sitemap 1) for the generation of the grid.
- A grid was generated in the 6MTU protein with X, Y, and Z coordinates 14.24, -16.52, and 25.87. The active site surrounded with the amino acid residues Chain A: LYS746, SER748, GLU792, HIS793, HIS794, VAL797, GLU798, ARG801; Chain B: LYS746, GLY747, SER748, GLU792, HIS793, HIS794, VAL797, GLU798, ARG801; Chain C: HIS823, ASN825, GLU826, THR827; Chain D: ASN825, GLU826, THR827.
- A grid was generated in the 6YQ4 protein with X, Y, and Z coordinates -34.27, -41.36, and -43.8. The active site surrounded with the amino acid residues Chain B: ILE22, ASN23, PRO76, ASN77, THR78, VAL79, ASP88, GLY93, ASP95, LYS97, ALA98, ASN99, SER100, LEU101, TYR103, ASN163, GLY164, THR165, GLY168, TYR206, MET222, TYR223, ARG231, MET232, GLU241, ASN244, ASP245, ARG246, SER247, LEU248, THR249, ARG250, THR252, ILE307, PHE324, LEU340, TYR343, THR344, ILE346, GLY347, ASP348, MET350, HIS440, GLY441, ALA442, ILE443, ASP444, LYS445, ASP446, SER448, LEU449, GLN474, GLY475, HIS476, GLY477, GLY478, ASP479, TYR480, ASP481, LEU482, GLU483, GLU484.
- The ligand preparation involves the conversion of 2D to 3D structures and producing their low energy states in Maestro format using an OPLS4 force field, with the possibility to extend each input structure by generating variation on ionization states.
- Finally docking was carried out using Glide software with standard precision and write SP descriptor information. During this procedure, favorable ligand poses were then generated to determine their spatial fit into the active site of the receptor and those that fitted best were then evaluated and minimized for generating glide scores.
- The Glide score, hydrogen bonds, and π-π interaction formed with the surrounding amino acids were used to predict the binding affinities and proper alignment of these compounds at the active site of the receptor.

5	Catechin	-6.18	SER741, GLU826, SEP828
6	Gallocatechin	-5.79	SER741, GLU826, SEP828
7	5-Fluorouracil	-5.71	LYS746, HIS793, HIS823
8	Gallocatechin gallate	-5.52	TYR751, SER761, GLU826, SEP828
9	Theoflavin-3'-gallate	-5.42	GLU826, SEP828
10	6-Mercaptopurine	-5.28	SEP828
11	Camptothecin	-4.40	THR749, SEP828, PRO822
12	Vinblastine	-3.62	TYR751, SEP828
13	Cyclophosphamide	-3.01	GLU792, HIS793, HIS794, ARG 801

Table No.2.Docking Score and Interactions of Compounds against 6YQ4 Protein

S. No	Compound Name	Docking Score	Interactions
1	Theoflavin-3'-gallate	-8.58	ASP95, ALA98, ASN99, ASN244, ASP479
2	Theoflavin3-3'-digallate	-8.19	ARG246, THR249, SER251, THR252, GLN323, LYS445, ASP446
3	Theoflavin-3-gallate	-7.83	GLN323, LYS445, ASP446, GLN474, GLY475, HIS476
4	Theoflavin	-7.71	ASP88, ALA98, ASP245, GLN 241, GLY478, TYR480
5	Catechin	-7.09	GLU233, LYS351, SER352, GLU365, ASP360
6	Gallocatechin	-6.68	ASP88, ALA98, SER100, GLN241, ASP479
7	Catechin gallate	-6.24	GLU233, TYR243, LYS351, PRO354, GLU365
8	6-Mercaptopurine	-6.07	ILE443, LYS445
9	Gallocatechin gallate	-5.91	ASP88, LYS97, ALA98, ASN99, ASP245, GLY478, ASSP479
10	5-Fluorouracil	-5.32	ASP88, THR165, GLN241
11	Camptothecin	-4.99	ARG231, LEU359
12	Cyclophosphamide	-4.42	SER352, PRO354
13	Vinblastine	-4.02	ASP88, ASN99
14	Vincristine	-3.95	ASP348

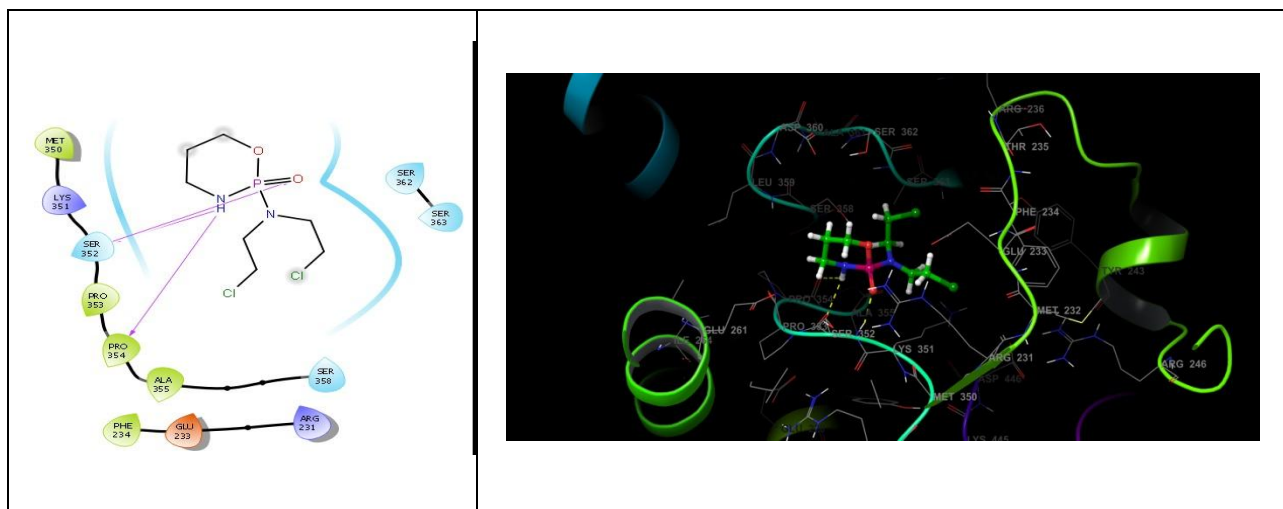


Figure No.2.2907- Molecular docking of glutamate ionotropic receptor NMDA type subunit associated protein 1 -2D&3D Structure

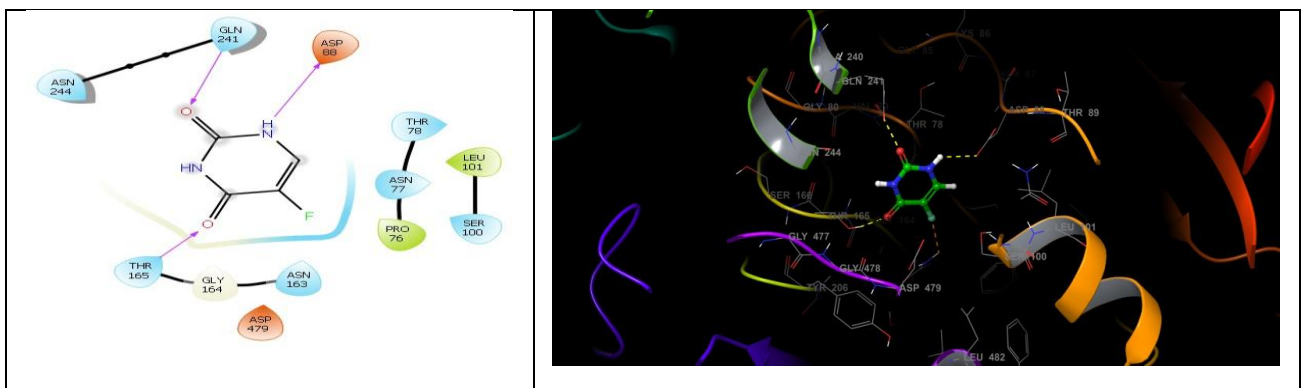


Figure No.3. 3385 - Molecular docking of Phospho NMDA Receptor Polyclonal antibody 2D&3D Structure

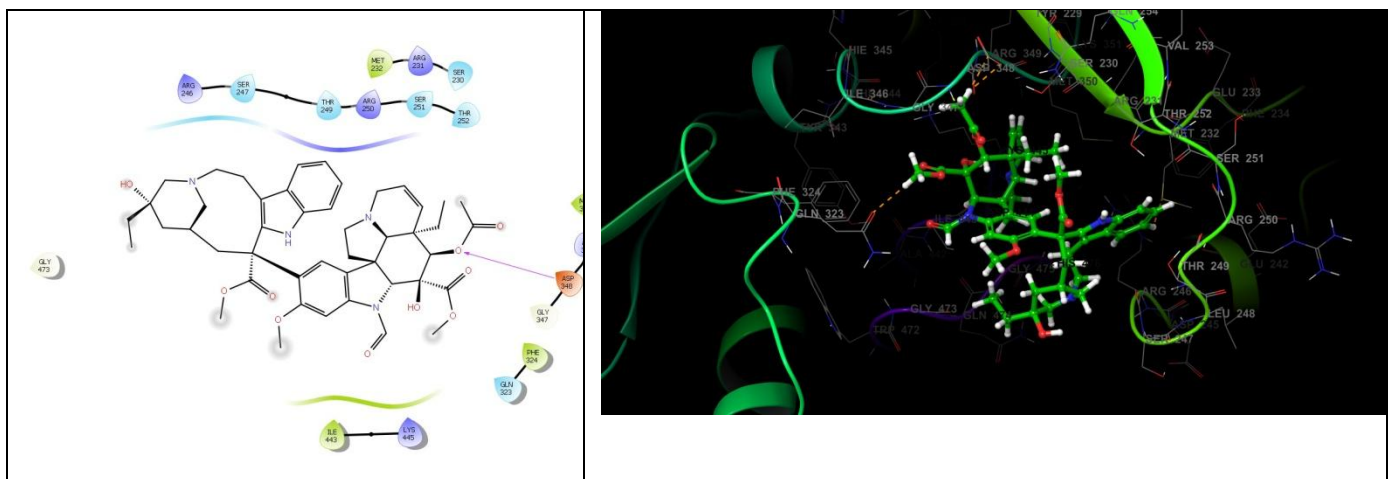
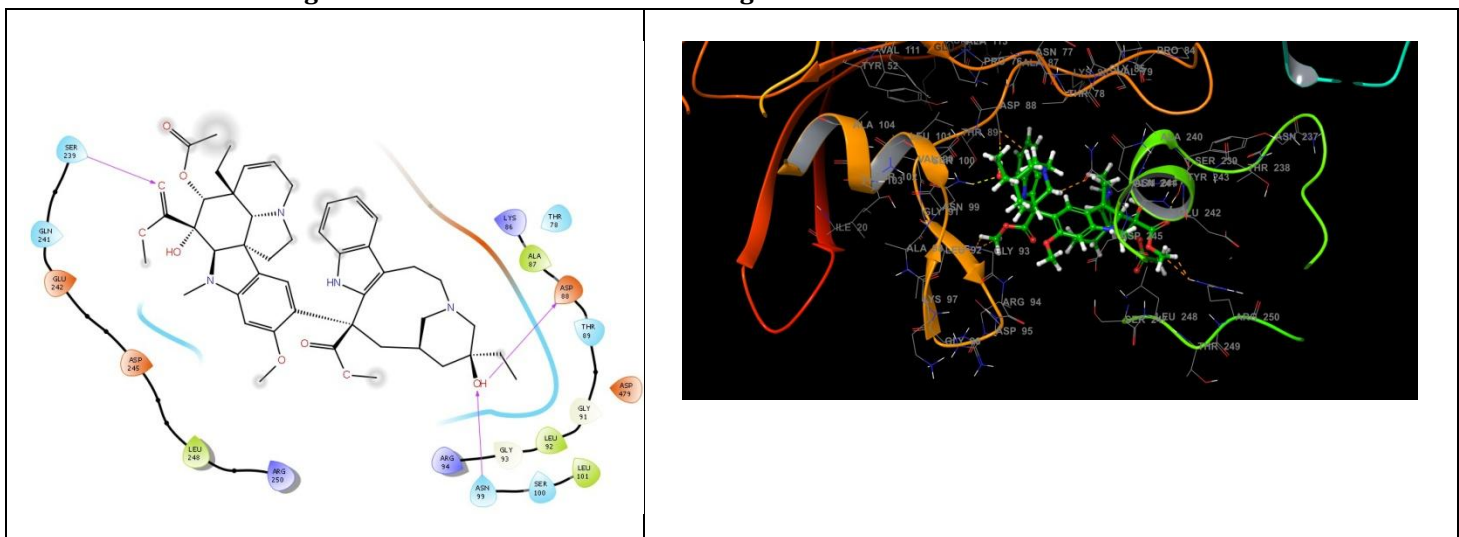


Figure No.4.5978 – Molecular docking of Interleukin IL-15RA Receptor sub unit- α 2D&3D Structure

Figure No.5.13342 - Molecular docking of Landiolol-2D&3D Structure



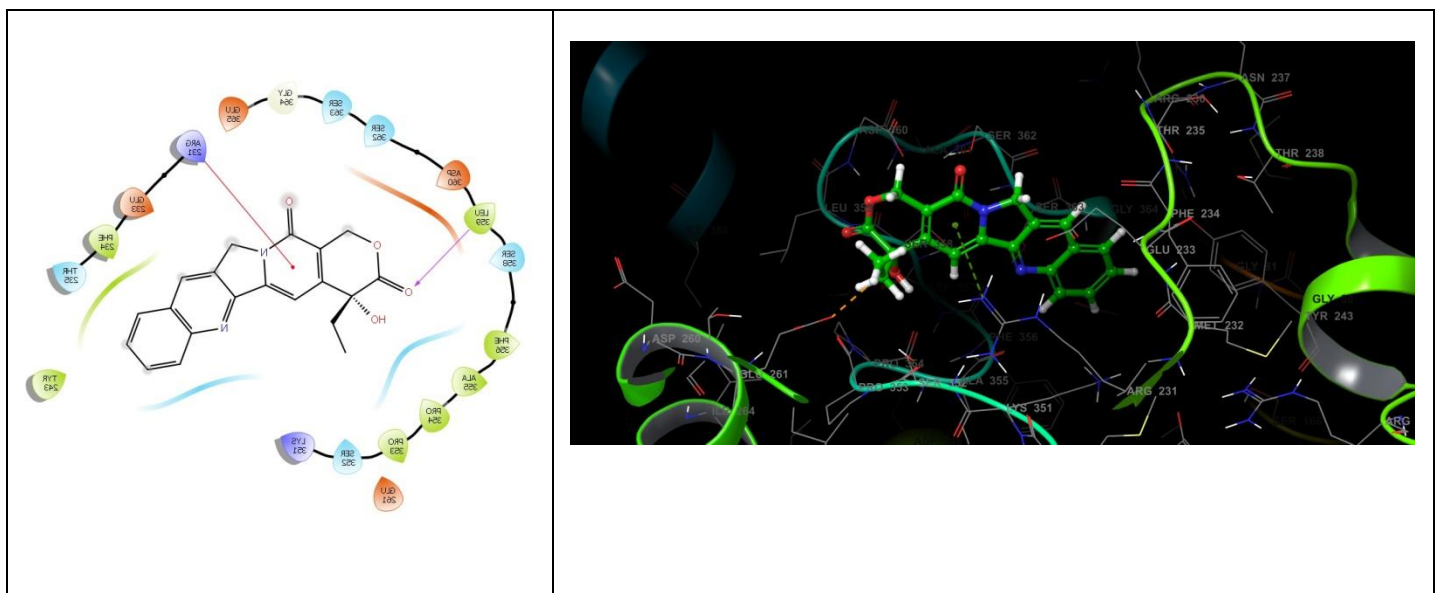


Figure No.6. 24360- Molecular docking of fatty acid binding proteins 1 -2D&3D Structure

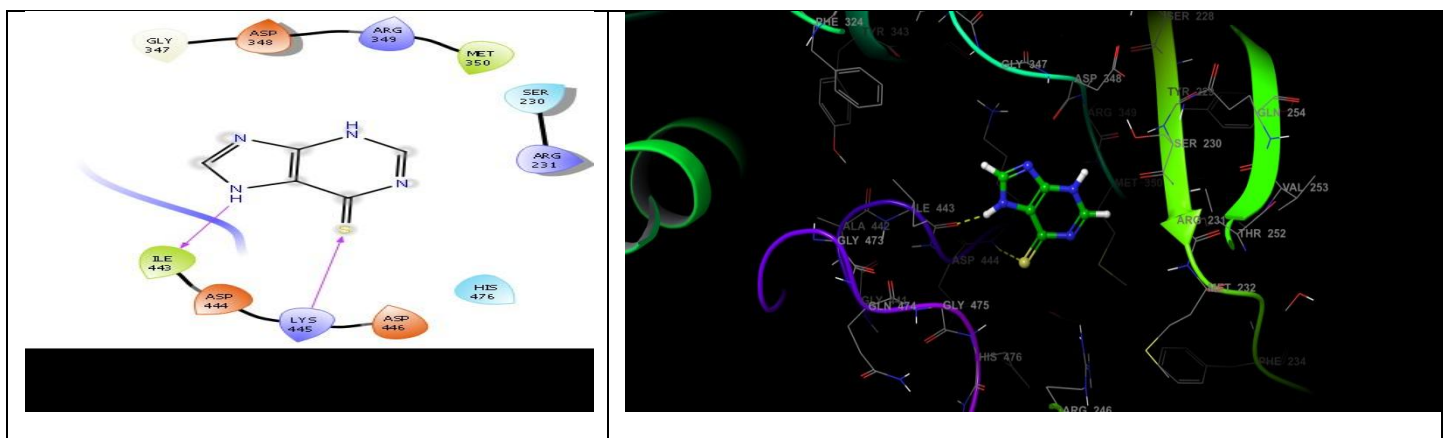


Figure No.7.667490 - Molecular docking of Mercapto purine 2D&3D Structure

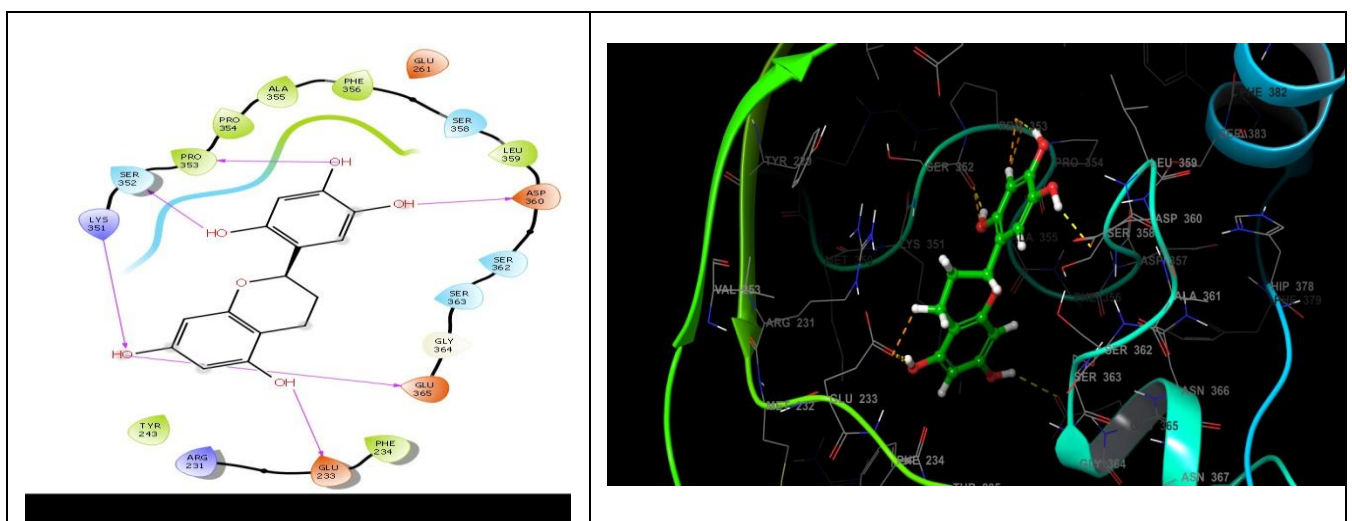


Figure No.8. Molecular docking of catechin -2D&3D Structure

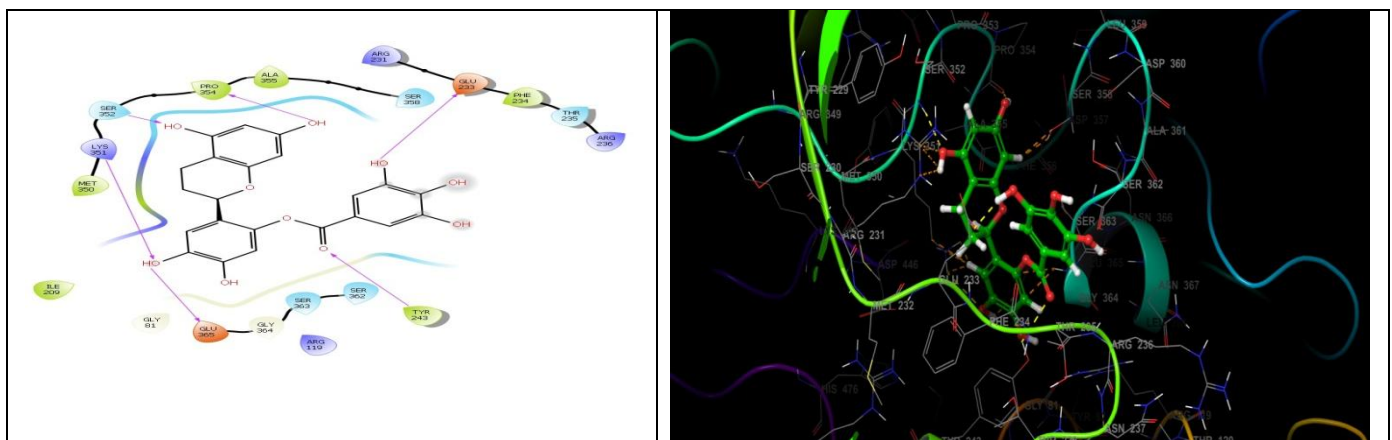


Figure No.9.Molecular docking of catechin gallate -2D&3D Structure

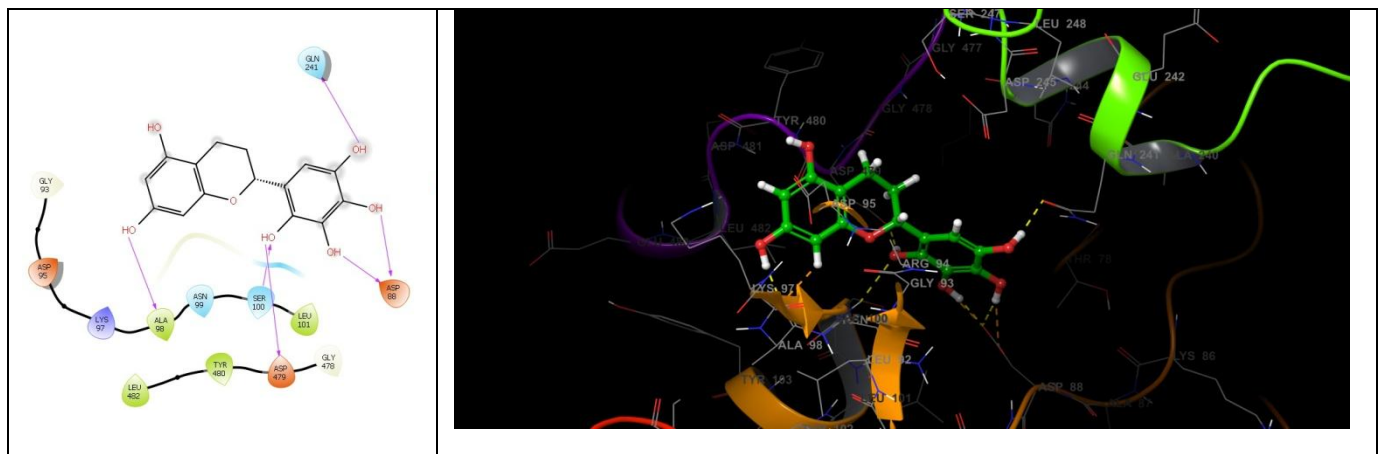


Figure No.10. Molecular docking of Gallo catechin -2D&3D Structure

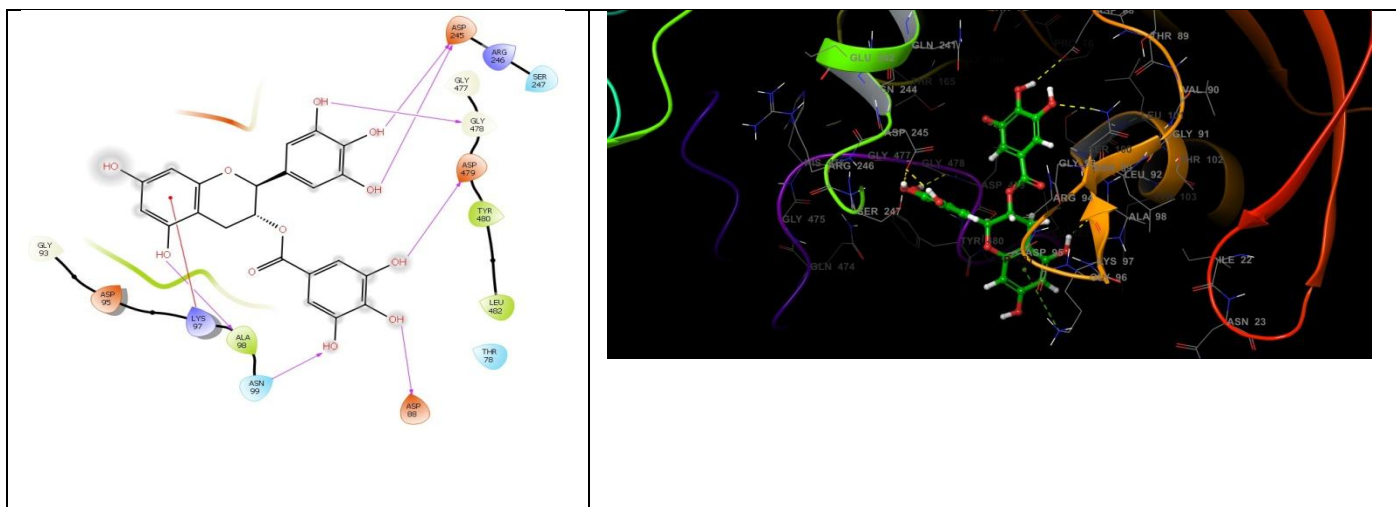


Figure No.11. Molecular docking of Gallo catechin gallate -2D&3D Structure

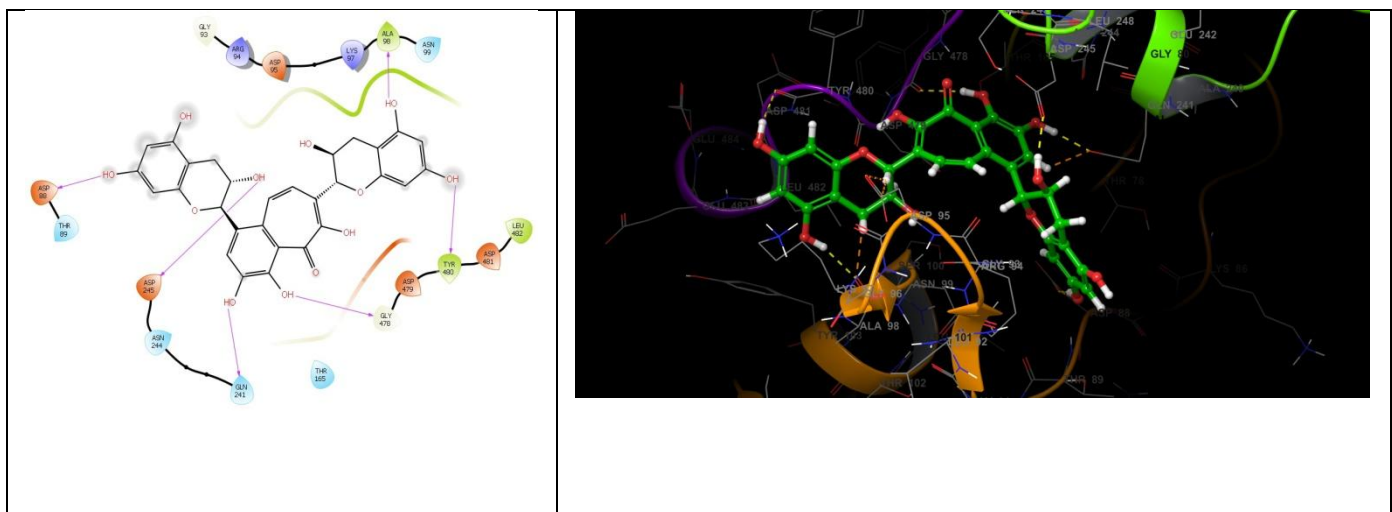


Figure No.12.Molecular docking of Theofalvin-2D&3D Structure

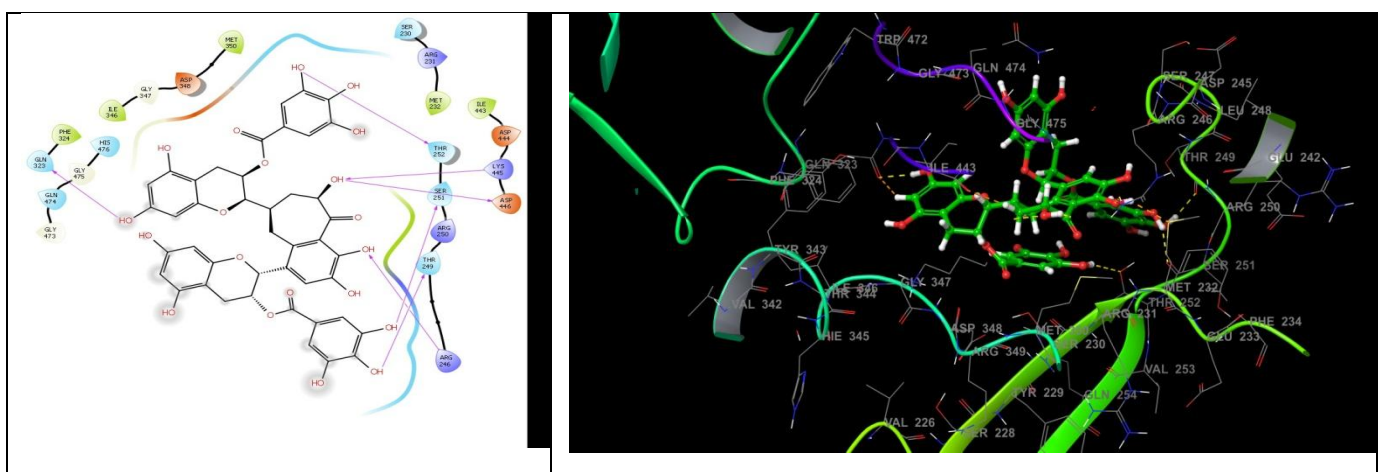


Figure No.13.Molecular docking of Theoflavin 3-3¹ 2D&3D Structure

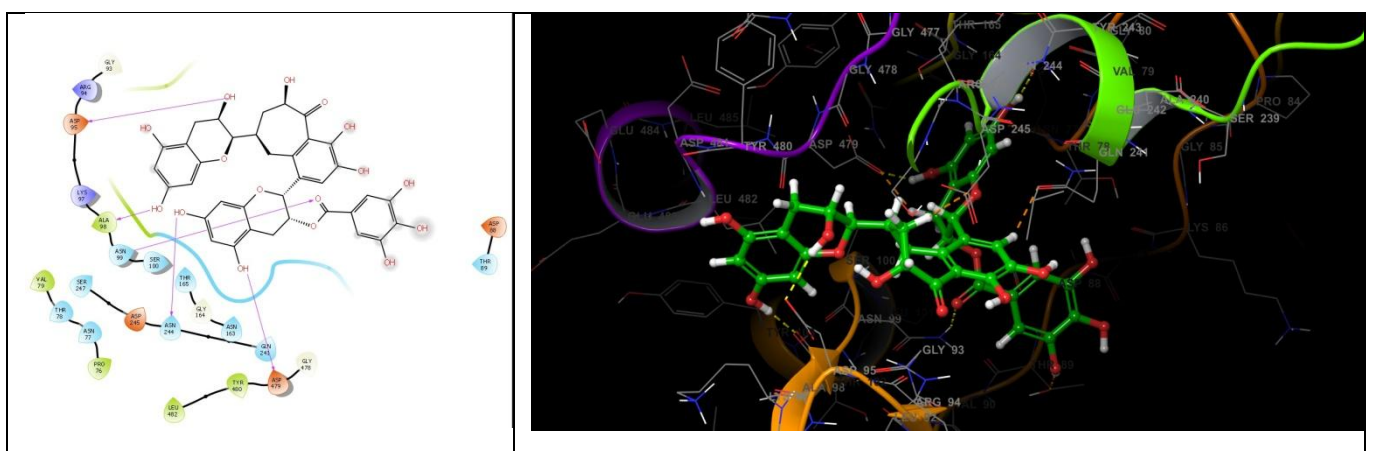


Figure No.14.Molecular docking of Theofalvin-3¹ gallate 2D&3D Structure

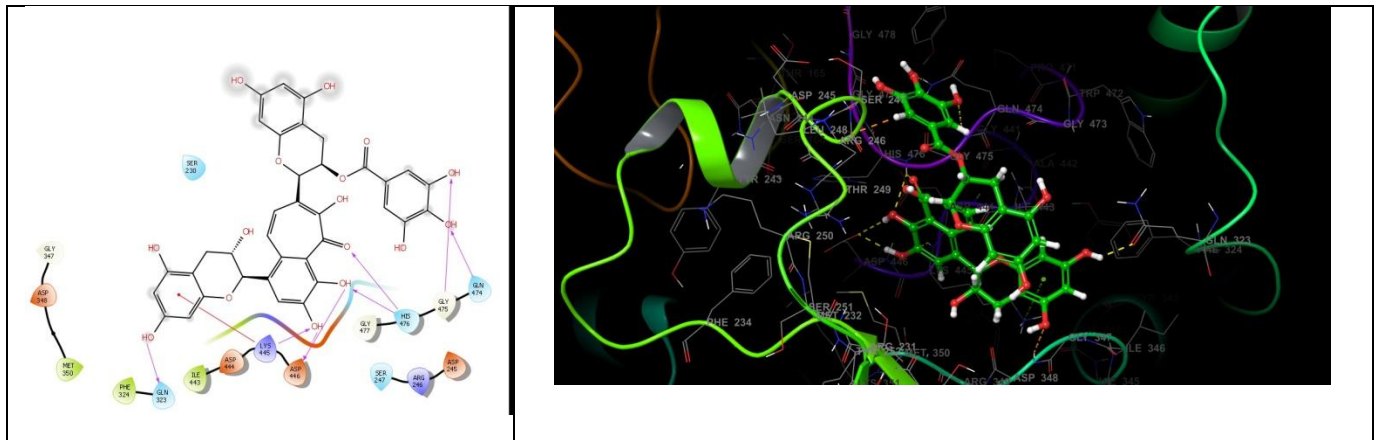


Figure No.15.Molecular docking of Theofalvin-3 gallate 2D&3D Structure

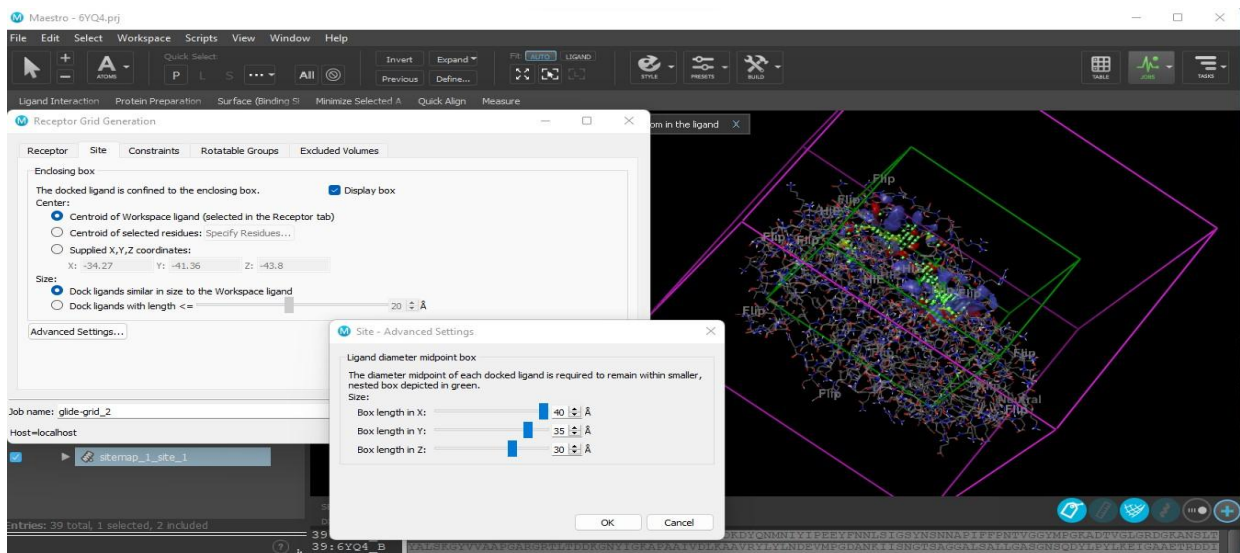


Figure NO.16.Docking

2.3. Preparation of Test Compound:

For MTT assay, Each Test compounds were weighed separately and dissolved in DMSO. With media make up the final concentration to 1 mg/ ml and the cells were treated with series of concentrations from 10 to 100 μ g/ ml.

3. MTT ASSAY:

3.1 Principle:

MTT Assay is a colorimetric assay that measures the reduction of yellow 3-(4,5-dimethylthiazol- 2-yl)-2,5-diphenyl tetrazolium bromide (MTT) by mitochondrial succinate dehydrogenase. The assay depends both on the number of cells present and, on the assumption, that dead cells or their products do not reduce tetrazolium. The MTT enters the cells and passes into the mitochondria where it is reduced to an insoluble, dark purple colored formazan crystals. The cells are then solubilized with a DMSO and the released, solubilized formazan reagent is measured spectrophotometrically at 570 nm.

3.2 Procedure:

Cell viability was evaluated by the MTT Assay with three independent experiments with five concentrations of compounds in triplicates. Cells were trypsinized and perform the trypan blue assay to know viable cells in cell suspension. Cells were counted by haemocytometer and seeded at density of 5.0×10^3 cells / well in 100 μ l media in 96 well plate culture medium and incubated overnight at 37 °C. After incubation, take off the old media and add fresh media 100 μ l with different concentrations of test compound in represented wells in 96 plates. After 48 hrs., Discard the drug solution and add the fresh medic with MTT solution (0.5 mg / mL-1) was added to each well and plates were incubated at 37 °C for 3 hrs. At the end of incubation time, precipitates are formed as a result of the reduction of the MTT salt to chromophore formazan crystals by the cells with metabolically active mitochondria. The optical density of solubilized crystals in DMSO was measured at 570 nm on a microplate reader. The percentage growth

inhibition was calculated using the following formula.

$$\% \text{ Inhibition} = \frac{100 (\text{Control} - \text{Treatment})}{\text{Control}}$$

The IC_{50} value was determined by using linear regression equation i.e. $Y = Mx + C$. Here, $Y = 50$, M and C values were derived from the viability graph.

4.1.a Twigs Methanolic :

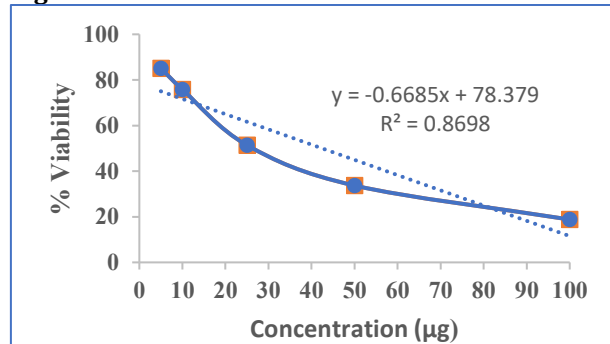
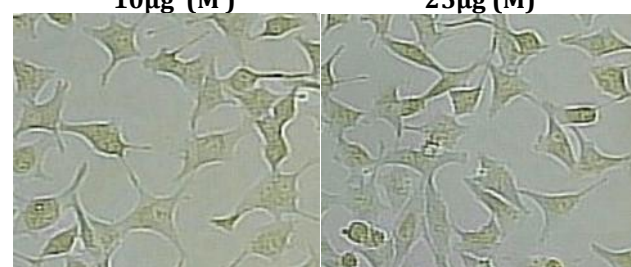
Table -3

Concentration (μg)	Absorbance at 570nm	% Inhibition	% Viability	IC_{50} (μg)
5	0.394	14.9	85.1	42.45 ± 0.754
10	0.342	26.13	75.87	
25	0.238	48.59	51.41	
50	0.156	66.3	33.7	
100	0.087	81.2	18.8	
Untreated	0.463	0	100	
Blank	0	0	0	

Table -4

Concentration (μg)	% Viability
5	85.1
10	75.87
25	51.41
50	33.7
100	18.8

Figure -17

5 μg (M)10 μg (M)25 μg (M)50 μg (M) 100 μg (M)
Figure no -18 .Methanolic twigs

4.1.bTwigs Ethyl acetate:

Table -5

Concentration (µg)	Absorbance at 570nm	% Inhibition	% Viability	IC ₅₀ (µg)
5	0.426	7.99	92.01	60.46±0.913
10	0.374	19.22	80.78	
25	0.297	35.85	64.15	
50	0.212	54.21	45.79	
100	0.153	66.95	33.05	
Untreated	0.463	0	100	
Blank	0	0	0	

Table -6

Concentration (µg)	% Viability
5	92.01
10	80.78
25	64.15
50	45.79
100	33.05

Figure-19

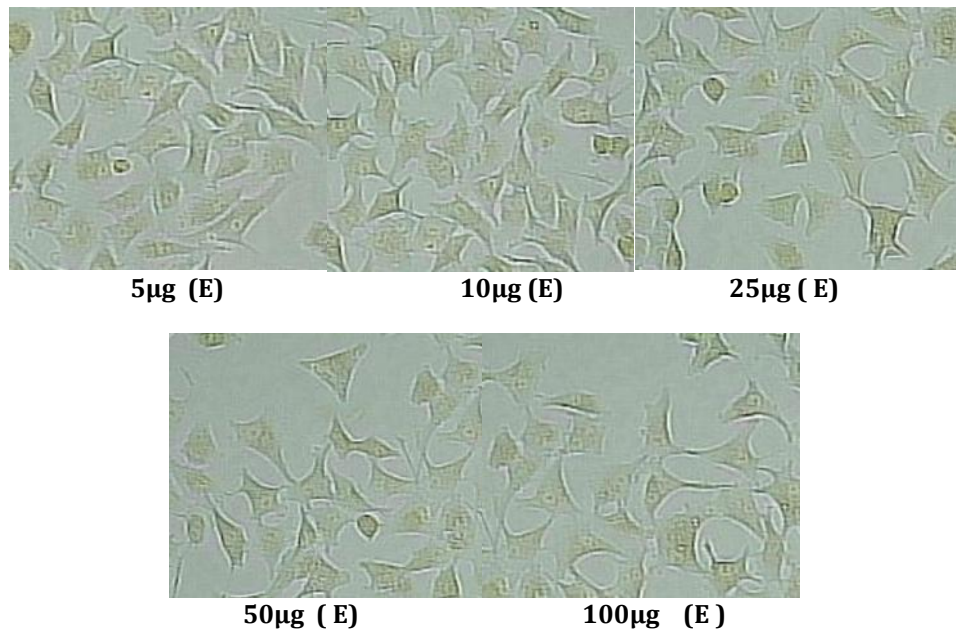
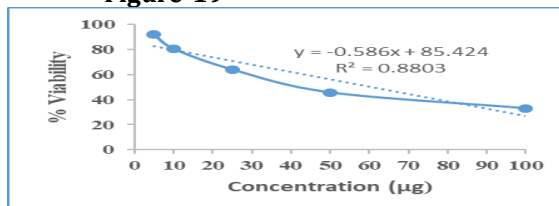


Figure no:20 Ethyl acetate Twigs

4.1. Twigs Hexane :

Table-7

Concentration (µg)	Absorbance at 570nm	% Inhibition	% Viability	IC ₅₀ (µg)
5	0.448	3.23	96.77	86.73±1.587
10	0.422	8.85	91.15	
25	0.374	19.22	80.78	
50	0.295	36.28	63.72	
100	0.213	53.99	46.01	
Untreated	0.463	0	100	

Blank	0	0	0	
-------	---	---	---	--

Table-8

Concentration (μg)	% Viability
5	96.77
10	91.15
25	80.78
50	63.72
100	46.01

Figure-21

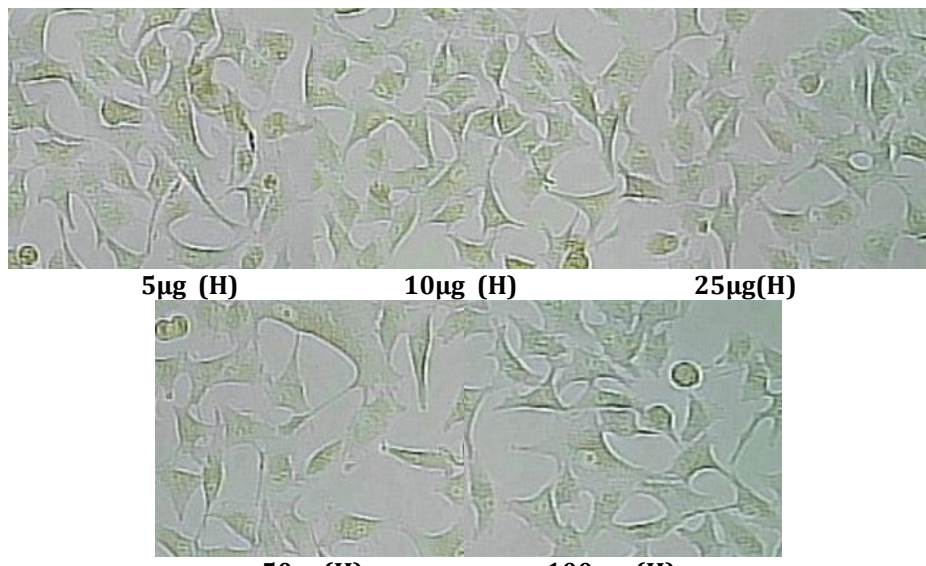
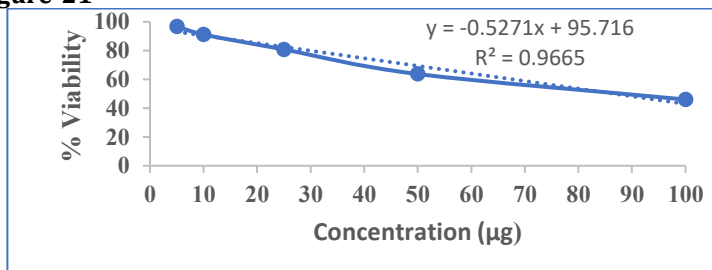


Figure no -22.Heaxane Twigs

4. 1.d.Twigs Butanolic :

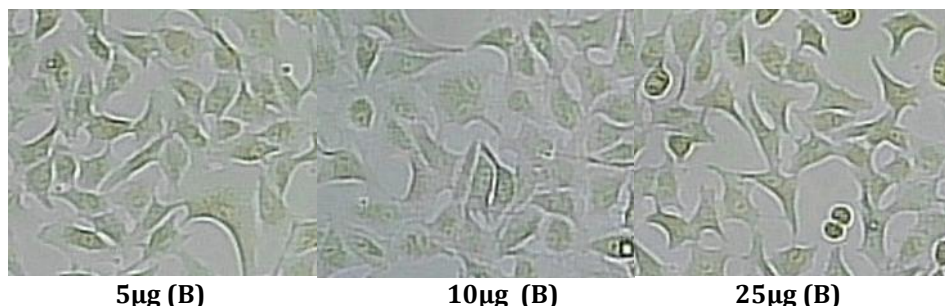
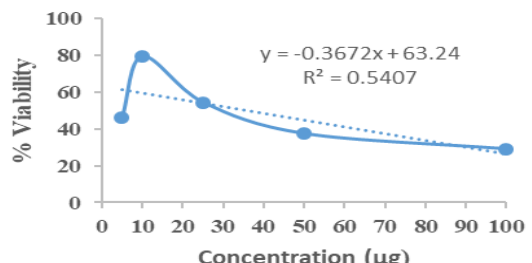
Table-9

Concentration (μg)	Absorbance at 570nm	% Inhibition	% Viability	IC ₅₀ (μg)
5	0.411	11.23	46.19	
10	0.368	20.51	79.49	
25	0.252	45.57	54.43	
50	0.173	62.63	37.37	
100	0.134	71.05	28.95	
Untreated	0.463	0	100	36.05±0.614
Blank	0	0	0	

Table-10

Figure -23

Concentration (μ g)	% Viability
5	46.19
10	79.49
25	54.43
50	37.37
100	28.95



S. No	SAMPLE NAME	IC50 (μ g)
		MCF 7
1	TM	42.45 \pm 0.754
2	TE	60.46 \pm 0.913
3	TH	86.73 \pm 1.587
4	TB	36.05 \pm 0.614
5	Cisplatin(μ M)	5.78 \pm 0.126

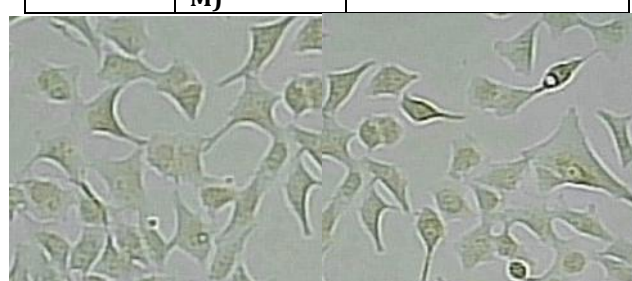


Figure no -24. Butanolic twigs

SUMMARY :

Test compounds treated with MCF 7, HepG2 cells showing the IC 50 values are as follow in the table provided

Summary and Conclusion:

This study evaluated the cytotoxic potential of different solvent extracts (methanolic, butanolic, hexane, and ethanolic) derived from *Camellia sinensis* twigs using MTT assay and in silico molecular docking. The results revealed that the methanolic extract exhibited the highest cytotoxic activity, particularly against MCF-7 breast cancer cells, with the lowest IC50 value. Butanolic and ethanolic extracts also showed moderate cytotoxic

effects, whereas hexane extract had the least activity.

Molecular docking studies demonstrated strong binding interactions of the extracted compounds with target proteins (6MTU and 6YQ4), indicating their potential anticancer mechanisms. Notably, catechin gallate and theaflavins exhibited the most promising docking scores, suggesting their role in inhibiting cancer cell proliferation.

In conclusion, the findings highlight the potential of *Camellia sinensis* twig extracts as promising sources of bioactive compounds for anticancer applications. Further studies, including in vivo investigations and compound isolation, are essential to validate their therapeutic efficacy and safety.

References:

1. Graham H.N. Green tea composition, consumption, and polyphenol chemistry. *Prev. Med.* 1992; 21:334-350. doi: 10.1016/0091-7435(92)90041-F.
2. Yamamoto T., Juneja L.R., Chu D., Kim M. *Chemistry and Applications of Green Tea.* CRC Press; Boca Raton, FL, USA: 1997. pp. 6-34.
3. Vuong Q.V., Stathopoulos C.E., Nguyen M., Golding J.B., Roach P.D. Isolation of green tea catechins and their utilization in the food industry. *Food Rev. Int.* 2011; 27:227-247. doi: 10.1080/87559129.2011.563397.
4. Khalatbary A.R., Khademi E. The green tea polyphenolic catechin epigallocatechin gallate and neuroprotection. *Nutr. Neurosci.* 2018; 25:1-14. doi: 10.1080/1028415X.2018.1500124.
5. Sudano Roccaro A, Blanco AR, Giuliano F, Rusciano D, Enea V. Epigallocatechin-gallate enhances the activity of tetracycline in staphylococci by inhibiting its efflux from bacterial cells. *Antimicrob Agents Chemother.* 2004; 48:1968-1973. doi: 10.1128/AAC.48.6.1968-1973.2004.
6. Graham HN. Green tea composition, consumption, and polyphenol chemistry. *Prev Med.* 1992; 21:334-350. doi: 10.1016/0091-7435(92)90041-F.
7. K. Kaihatsu, M. Yamabe, and Y. Ebara, "Antiviral mechanism of action of epigallocatechin-3-O-gallate and its fatty acid esters," *Molecules*, vol. 23, no. 10, p. 2475, 2018.
8. K. Jakubczyk, J. Kochman, A. Kwiatkowska et al., "Antioxidant properties and nutritional composition of matcha green tea," *Foods*, vol. 9, no. 4, p. 483, 2020.
9. Yang CS, Wang H, Sheridan ZP. Studies on the bioavailability of tea polyphenols. *Curr Pharmacol Rep.* 2022;8(3):119-28.
10. Khan N, Mukhtar H. Tea polyphenols in promotion of human health. *Nutrients.* 2019;11(1):39.
11. Friedman M. Overview of antibacterial, antitoxin, antiviral, and antifungal activities of tea flavonoids and tannins. *Molecules.* 2007;12(7):1462-96.
12. Kumazoe M, Tachibana H. Green tea catechins in cancer chemoprevention: practical application. *Molecules.* 2021;26(15):4746.
13. Luo KW, Yue GG, Ko CH, Lee JK, Li KK, Lee M, et al. In vivo and in vitro investigation of the potential therapeutic effect of epigallocatechin gallate in colon cancer. *Nutrients.* 2020;12(11):3400.
14. Lopes RG, Machado MT, Alvarez M, Hubinger MD. Green tea polyphenols: encapsulation and application in food. *Food Chem.* 2021;334:127485.
15. Landis-Piwowar KR, Huo C, Chen D, Milacic V, Shi G, Chan TH, et al. Structure-activity relationships of green tea catechins on apoptosis in a human prostate cancer cell line. *Mol Cancer Ther.* 2007;6(3):818-27.
16. Singh BN, Shankar S, Srivastava RK. Green tea catechin, epigallocatechin-3-gallate (EGCG): mechanisms, perspectives and clinical applications. *Biochem Pharmacol.* 2011;82(12):1807-21.
17. Zhu Q, Huang Y, Li G, Guo W, Li J, Guo L, et al. Molecular docking and pharmacokinetic analysis of major green tea polyphenols as potential inhibitors of SARS-CoV-2 main protease. *Food Sci Nutr.* 2021;9(10):5890-901.
18. Kumar NB, Besterman-Dahan K, Kang L, Pow-Sang J, Xu P, Allen K, et al. Results of a randomized clinical trial evaluating the safety of green tea polyphenols for prostate cancer prevention. *Oncotarget.* 2020;11(42):3740-50.
19. Lambert JD, Elias RJ. The antioxidant and pro-oxidant activities of green tea polyphenols: a role in cancer prevention. *Arch Biochem Biophys.* 2010;501(1):65-72.
20. Musial C, Kuban-Jankowska A, Gorska-Ponikowska M. Beneficial properties of green tea catechins. *Int J Mol Sci.* 2020;21(5):1744.
21. Rendeiro C, Spencer JP, Vauzour D. The neuroprotective functions of flavonoids: mechanisms at the cellular and molecular levels. *Curr Med Chem.* 2015;22(23):2760-72.
22. Johnson R, Bryant S, Huntley AL. Green tea and green tea catechin extracts: an overview of the clinical evidence. *Maturitas.* 2021;143:15-24.
23. Thielecke F, Boschmann M. The potential role of green tea catechins in the prevention of the metabolic syndrome – a review. *Phytochemistry.* 2009;70(1):11-24.
24. Lee WJ, Shim JY, Zhu BT. Mechanisms for the inhibition of DNA methyltransferases by tea catechins and bioflavonoids. *Mol Pharmacol.* 2005;68(4):1018-30.
25. Sun H, Wang Y, Zhang J, Wang W, He W, Xiang L, et al. Green tea polyphenols inhibit *Mycobacterium tuberculosis* survival in macrophages via modulation of autophagy and apoptosis. *Food Chem Toxicol.* 2020;136:110961.

